Research Papers

GREENSUSMATER

Greensusmater
Vol. 2, No. 1, 2025
https://doi.org/10.62755/greensusmater.2025.2.1.1-6

Check for updates

Effect of Zeolite Mesh Size Variation on the Filtration Performance of Zeolite-PAN/PVDF Nanofiber for Methylene Blue Dye Removal

Dheace Gracesela Buya[1] Rizky Aflaha[2] Aditya Rianjanu[1,3]

[1] *Department of Materials Engineering, Faculty of Industrial Technology, Institut Teknologi Sumatera, Terusan Ryacudu, Way Hui, Jati Agung, Lampung Selatan, 35365 Indonesia*
[2] *Department of Physics, Faculty of Mathematics and Natural Sciences, Universitas Gadjah Mada, Sekip Utara PO Box BLS 21, Yogyakarta 55281, Indonesia*
[3] *Center for Green and Sustainable Materials, Institut Teknologi Sumatera, Terusan Ryacudu, Way Hui, Jati Agung, Lampung Selatan 35365, Indonesia*

Corresponding author: aditya.rianjanu@mt.itera.ac.id (AR)

ARTICLE HISTORY: Received: May 13, 2025 | Revised: May 30, 2025 | Accepted: June 10, 2025

ABSTRACT

Water pollution from industrial effluents, particularly synthetic dyes like methylene blue (MB), poses significant environmental challenges. Electrospun nanofiber membranes based on polyacrylonitrile (PAN) and polyvinylidene fluoride (PVDF) are promising for filtration due to their high surface area and porous structure. However, their limited dye adsorption capacity requires enhancement, which can be achieved by incorporating natural zeolite particles known for their high ion-exchange capacity. In this study, we developed Ze-PAN/PVDF nanofiber membranes using zeolite with varying particle sizes (mesh sizes 50, 100, 200, 300) via vacuum filtration and evaluated their performance in MB dye removal. All Ze-PAN/PVDF membranes exhibited high initial dye rejection (above 97%) in the first two cycles, while the control PAN/PVDF membrane showed minimal rejection, decreasing from 35% to 7% over five cycles. The decline in rejection efficiency became noticeable from the third cycle, with values of 67%, 39%, 74%, and 86% for Ze50, Ze100, Ze200, and Ze300, respectively. Permeation flux was significantly affected by zeolite particle size, with the PAN/PVDF membrane maintaining a high flux (>10,000 L m^{-2} h^{-1} bar^{-1}), while Ze50-PAN/PVDF dropped to 260 ± 30 L m^{-2} h^{-1} bar^{-1}. Finer particles in Ze300-PAN/PVDF maintained relatively higher flux (370 ± 200 L m^{-2} h^{-1} bar^{-1}), indicating reduced pore blockage. These findings highlight the importance of optimizing zeolite particle size to achieve high dye removal efficiency and stable flux, making Ze300-PAN/PVDF a promising candidate for wastewater treatment applications.

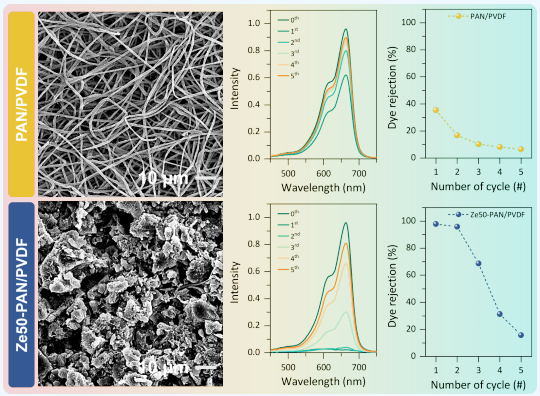

Keywords: *Ze-PAN/PVDF Nanofiber, Zeolite Particle Size, Methylene Blue Removal, Electrospun Membrane, Wastewater Treatment*

1. INTRODUCTION

Water pollution from industrial processes, particularly the discharge of synthetic dyes and other organic contaminants, remains a major environmental issue [1, 2]. These pollutants are often toxic, persistent, and resistant to natural degradation, posing risks to aquatic ecosystems and human health [3, 4]. Conventional water treatment methods, such as coagulation, chemical oxidation, and biological processes, often fall short in effectively removing dyes from wastewater, especially at low concentrations [5, 6]. Consequently, advanced filtration techniques are increasingly being explored to enhance pollutant removal efficiency [7, 8, 9].

Among various filtration technologies, nanofiber-based membranes have emerged as promising candidates due to their unique structural features [10, 11, 12]. Electrospun nanofiber membranes, typically composed of polymers like polyacrylonitrile (PAN) and polyvinylidene fluoride (PVDF), offer high porosity, interconnected pore networks, and large surface area-to-volume ratios [13, 14, 15, 16]. These characteristics facilitate efficient water permeability and increased contact with pollutants, making them suitable for dye removal applications. However, pure polymeric nanofibers may exhibit limited adsorption capacity for cationic dyes, such as methylene blue (MB), which restricts their effectiveness in practical applications.

To address this limitation, inorganic fillers like natural zeolite can be incorporated into the nanofiber matrix to enhance adsorption properties [17, 18]. Zeolite, a microporous aluminosilicate mineral, is widely known for its high ion-exchange capacity and affinity for cationic pollutants [19, 20, 21]. Integrating zeolite into PAN/PVDF nanofibers can improve dye removal efficiency through combined adsorption and filtration mechanisms [17, 18]. However, the size of zeolite particles plays a critical role in determining membrane performance. Larger particles may cause pore blockage, reducing flux, while finer particles are likely to disperse more uniformly, maintaining membrane porosity and enhancing contaminant capture [22, 23].

Despite the potential advantages, the effect of zeolite particle size on the filtration efficiency of nanofiber membranes

has not been thoroughly investigated. Therefore, this study aims to develop zeolite-modified PAN/PVDF nanofiber membranes using different zeolite particle sizes (mesh sizes 50, 100, 200, 300) and evaluate their filtration performance against methylene blue dye. By systematically analyzing dye rejection and permeation flux, this research seeks to identify the optimal zeolite configuration that balances high filtration efficiency with stable flux, contributing to the development of more effective filtration membranes for wastewater treatment.

2. MATERIALS AND METHODS

2.1 Materials

The primary materials used in this study were Polyacrylonitrile (PAN) and Polyvinylidene Fluoride (PVDF), both obtained from Sigma-Aldrich. PAN (Mw = 150,000 g/mol) and PVDF (Mw = 534,000 g/mol) were employed as the main polymer components for nanofiber fabrication. N,N-Dimethylformamide (DMF, $\geq$ 99%) from Merck was utilized as the solvent for polymer dissolution. Natural zeolite was sourced from Sumatera, Indonesia, and prepared in four different mesh sizes: 50, 100, 200, and 300. Methylene blue (MB) dye, used as a model pollutant, was also acquired from Merck. The prepared nanofiber samples were designated based on the zeolite mesh size as follows: Ze50-PAN/PVDF, Ze100-PAN/PVDF, Ze200-PAN/PVDF, Ze300-PAN/PVDF, and PAN/PVDF (control sample without zeolite).

2.2 Preparation of PAN/PVDF nanofiber

The PAN/PVDF nanofiber membranes were prepared using the electrospinning technique. Initially, 1 g of PAN was dissolved in 10 mL of DMF under continuous stirring at 60°C for 2 hours to ensure complete dissolution. Afterward, 0.25 g of PVDF was added to the mixture, and the solution was stirred for an additional 2 hours to achieve a homogeneous blend. The resulting polymer solution was transferred to a 10 mL syringe fitted with a stainless-steel needle. The electrospinning process was performed using a digital electrospinner (ILMI-N101 Electrospinning) with the following parameters: a high voltage of 9 kV, a tip-to-collector distance of 15 cm, and a flow rate of 0.5 mL/h. Electrospinning was conducted for 10 hours to form nanofiber membranes.

2.3 Preparation of Ze-PAN/PVDF membrane

To incorporate zeolite into the PAN/PVDF nanofiber membranes, natural zeolite was first ground and sieved to obtain particles of four different sizes corresponding to mesh numbers 50, 100, 200, and 300 using Mini-sieve micro sieve set (Sigma-Aldrich). The sieved zeolite was thoroughly washed with deionized water to eliminate any surface contaminants and dried at 100°C for 24 hours. The dried zeolite was then dispersed in deionized water at a concentration of 0.03 g per 100 mL and subjected to ultrasonication for 30 minutes to ensure uniform particle dispersion. The PAN/PVDF nanofiber membrane was cut into square pieces (30 × 30 mm) and mounted on a vacuum filtration apparatus (Sigma-Aldrich® vacuum filtration assembly). The dispersed zeolite suspension was poured onto the nanofiber surface and subjected to vacuum filtration at 0.5 bar to uniformly coat the nanofiber membrane with zeolite particles. The zeolite-coated PAN/PVDF membranes were designated according to the mesh size of the zeolite used: Ze50-PAN/PVDF, Ze100-PAN/PVDF, Ze200-PAN/PVDF, and Ze300-PAN/PVDF.

2.4 Materials characterizations

The morphological structure of the PAN/PVDF and Ze-PAN/PVDF membranes was analyzed using Scanning Electron Microscopy (SEM-EDX, model JEOL JSM-6510) to evaluate fiber diameter, surface topology, and zeolite distribution within the nanofibers. Energy Dispersive X-ray Spectroscopy (EDS) was employed to identify the elemental composition and verify the presence of zeolite on the membrane surface. Fourier Transform Infrared Spectroscopy (FTIR, Shimadzu IRSpirit-X Compact FTIR Spectrometer.) was conducted to detect characteristic functional groups and confirm successful incorporation of zeolite into the nanofiber matrix.

2.5 Filtration investigations

The filtration performance of the PAN/PVDF and Ze-PAN/PVDF membranes was evaluated using a vacuum filtration system. Each membrane, cut into a 30 × 30 mm square, was placed in a filtration holder connected to a vacuum pump set to maintain a pressure of 0.5 bar. The model pollutant used for testing was a methylene blue (MB) dye solution prepared at a concentration of 5 ppm. A volume of 25 mL of the dye solution was filtered through each membrane during each filtration cycle. The permeate was collected after each filtration cycle, and the residual dye concentration was measured using a UV-Vis spectrophotometer (Shimadzu UV-1280) at a wavelength of 664 nm. The filtration process was repeated for five consecutive cycles to evaluate the stability and reusability of the membranes. The dye rejection efficiency (R) was calculated as the percentage reduction in dye concentration between the feed and permeate solutions, using the formula in Eq. (1):

$$R(\%) = \frac{(C_0 - C_t)}{C_0} \times 100 \quad (1)$$

Where C_0 is the initial dye concentration (ppm) and Ct is the dye concentration after filtration (ppm). The permeate flux (J) was calculated using the following Eq. (2):

$$J_w = \frac{V}{t \times A \times P} \quad (2)$$

Where J is the permeate flux (L m^{-2} h^{-1} bar^{-1}), V is the volume of permeate collected (L), t is the filtration time (h), A is the membrane area (m^2), and P is the applied pressure (bar). To assess the durability and efficiency over prolonged use, the filtration performance metrics, including dye rejection and permeate flux, were recorded after each cycle. The stability of the membranes was evaluated by analyzing the consistency of rejection efficiency and flux across multiple filtration cycles.

3. RESULTS AND DISCUSSION

3.1 Ze-PAN/PVDF nanofiber characteristics

The surface morphology of PAN/PVDF and Ze-PAN/PVDF membranes with varying zeolite mesh sizes (i.e., 50, 100, 200, and 300) was analyzed using Scanning Electron Microscopy (SEM), as shown in Figure 1a. The PAN/PVDF membrane exhibited smooth and uniform fibrous structures typical of electrospun nanofibers. In contrast, all Ze-PAN/PVDF membranes displayed distinct morphological changes, characterized by the presence of zeolite particles dispersed across the nanofiber surfaces. As the mesh size increased (indicating a decrease in zeolite particle size), finer zeolite particles were more uniformly distributed, with Ze200 and Ze300 samples showing well-integrated particles within the nanofiber matrix.

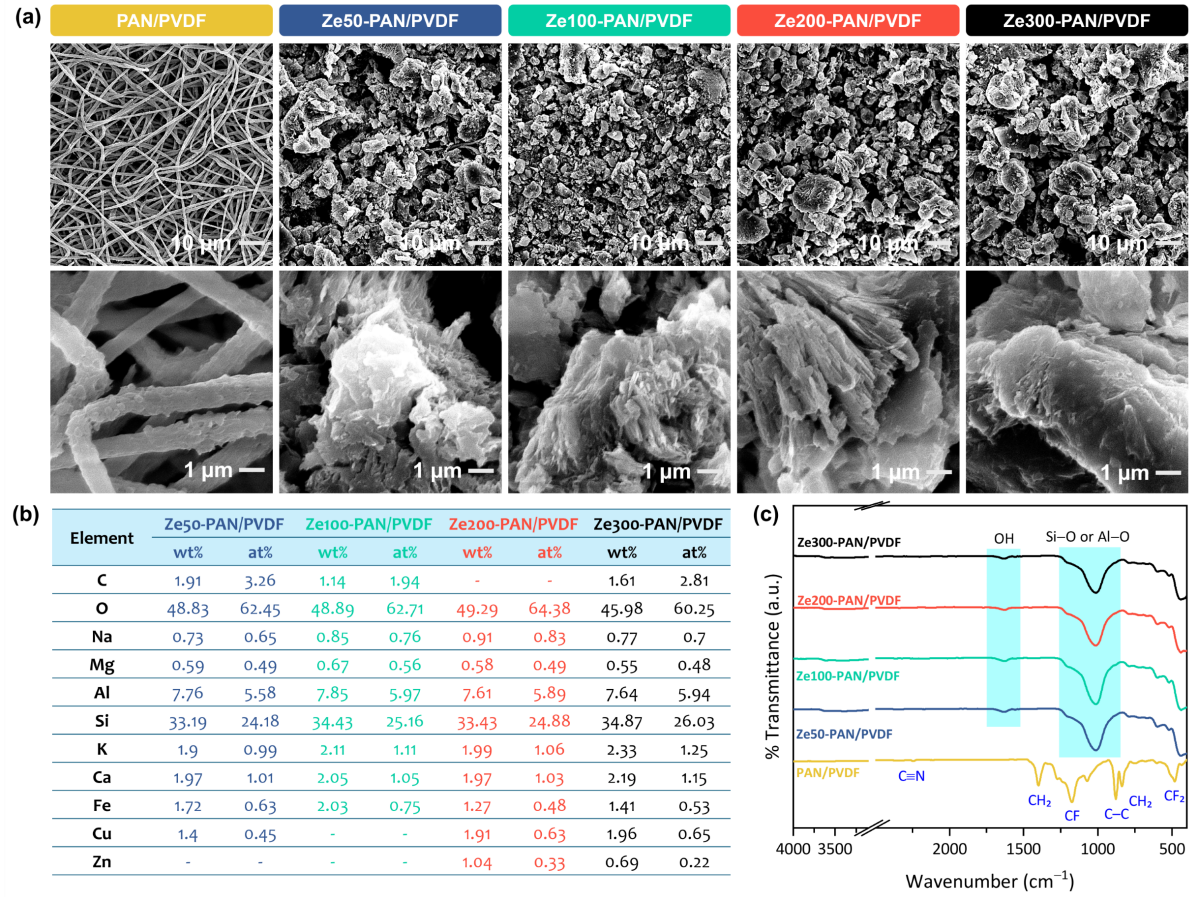

Element	Ze50-PAN/PVDF		Ze100-PAN/PVDF		Ze200-PAN/PVDF		Ze300-PAN/PVDF	
	wt%	at%	wt%	at%	wt%	at%	wt%	at%
C	1.91	3.26	1.14	1.94	-	-	1.61	2.81
O	48.83	62.45	48.89	62.71	49.29	64.38	45.98	60.25
Na	0.73	0.65	0.85	0.76	0.91	0.83	0.77	0.7
Mg	0.59	0.49	0.67	0.56	0.58	0.49	0.55	0.48
Al	7.76	5.58	7.85	5.97	7.61	5.89	7.64	5.94
Si	33.19	24.18	34.43	25.16	33.43	24.88	34.87	26.03
K	1.9	0.99	2.11	1.11	1.99	1.06	2.33	1.25
Ca	1.97	1.01	2.05	1.05	1.97	1.03	2.19	1.15
Fe	1.72	0.63	2.03	0.75	1.27	0.48	1.41	0.53
Cu	1.4	0.45	-	-	1.91	0.63	1.96	0.65
Zn	-	-	-	-	1.04	0.33	0.69	0.22

Figure 1. (a) Scanning Electron Microscopy (SEM) images of PAN/PVDF and Ze-PAN/PVDF nanofiber membranes with varying zeolite mesh sizes (50, 100, 200, 300). (b) Elemental composition analysis of Ze-PAN/PVDF membranes using Energy Dispersive X-ray Spectroscopy (EDS). (c) Fourier Transform Infrared (FTIR) spectra of PAN/PVDF and Ze-PAN/PVDF membranes.

In contrast, larger particles (Ze50 and Ze100) tend to cluster on the surface, forming aggregates rather than embedding within the fibers. This suggests that smaller zeolite particles result in more homogeneous dispersion, which could improve filtration performance [24, 25]. Energy Dispersive X-ray Spectroscopy (EDS) analysis, presented in Figure 1b, confirmed the presence of key elements, including carbon (C), oxygen (O), silicon (Si), aluminum (Al), sodium (Na), and magnesium (Mg), consistent with the PAN/PVDF matrix and zeolite composition [18]. Notably, the elemental composition was consistent across all Ze-PAN/PVDF samples, regardless of mesh size, indicating that the incorporation of differently sized zeolite particles did not significantly alter the chemical composition of the membranes. The consistent elemental profile suggests that the improved particle distribution observed in the smaller mesh size samples is purely due to physical dispersion rather than changes in the membrane's material composition.

The chemical structure of the PAN/PVDF and Ze-PAN/PVDF membranes was further analyzed using Fourier Transform Infrared (FTIR) spectroscopy, as shown in Figure 1c. The PAN/PVDF membrane exhibited characteristic peaks corresponding to the $-C\equiv N$ stretching vibration at around 2240 cm^{-1} and $-CH_2$ bending from PVDF around 1400 cm^{-1}. After incorporating zeolite, additional absorption bands appeared between 1000 and 1100 cm^{-1}, associated with the Si-O-Si and Al-O-Si stretching vibrations characteristic of zeolite. These new peaks confirmed the successful integration of zeolite particles within the PAN/PVDF matrix. The consistent appearance of these bands across different zeolite mesh sizes demonstrates that the incorporation of zeolite does not chemically alter the PAN/PVDF structure but rather enhances its functional properties through improved surface characteristics.

3.2 Ze-PAN/PVDF nanofiber filtration performance

The filtration performance of PAN/PVDF and Ze-PAN/PVDF membranes were evaluated using methylene blue (MB) dye as a model pollutant. The UV-Vis spectrum of MB shows a characteristic peak with the highest intensity at a wavelength of 664 nm. As shown in Figure 2a, the PAN/PVDF membrane (control sample) exhibited only a slight decrease in MB intensity after each filtration cycle, indicating minimal dye removal. In contrast, all Ze-PAN/PVDF membranes demonstrated a significant decrease in MB intensity, particularly during the first filtration cycle. This indicates that the incorporation of zeolite markedly enhances the dye adsorption capability of the membranes. Figure 2b shows the corresponding dye rejection (R) values for all membranes, calculated using Eq. (1). The PAN/PVDF membrane exhibited a minimal rejection value of 35% during the first cycle, which gradually decreased to 7% after the fifth cycle, highlighting its

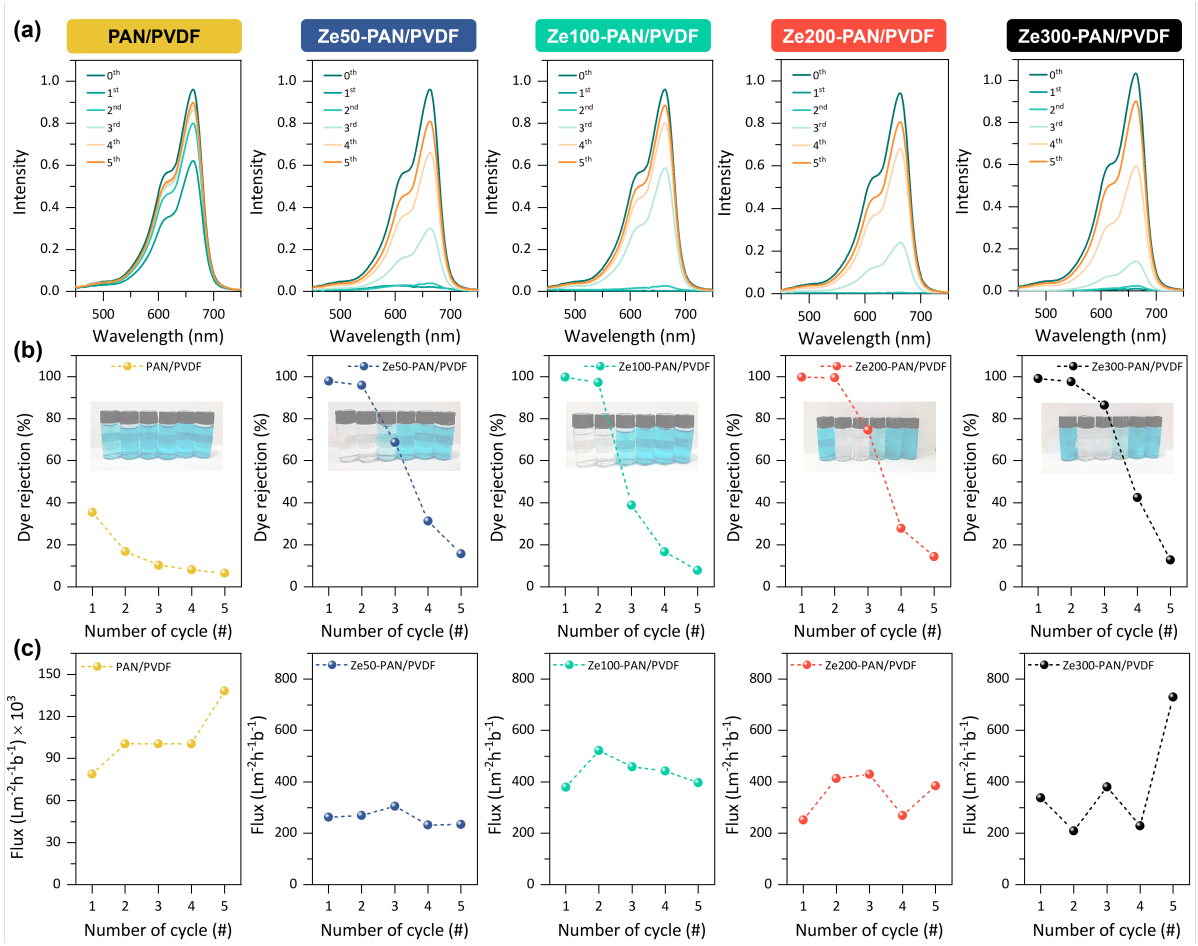

Figure 2. (a) UV-Vis spectra of methylene blue (MB) dye solutions after filtration through PAN/PVDF and Ze-PAN/PVDF membranes (Ze50, Ze100, Ze200, Ze300) over five filtration cycles, demonstrating the decrease in dye concentration. (b) Dye rejection percentage of each membrane during repeated filtration cycles, showing the gradual decline in filtration efficiency. (c) Permeate flux of PAN/PVDF and Ze-PAN/PVDF membranes across five filtration cycles, indicating variations in flux stability and performance consistency over repeated.

limited dye removal efficiency. In contrast, all Ze-PAN/PVDF membranes showed nearly complete dye removal in the first cycle, with rejection rates exceeding 97%. This near-complete removal efficiency was maintained throughout the second cycle as well. However, a significant decrease in dye rejection was observed from the third cycle onward. Specifically, the rejection values at the third cycle dropped to 67%, 39%, 74%, and 86% for Ze50-PAN/PVDF, Ze100-PAN/PVDF, Ze200-PAN/PVDF, and Ze300-PAN/PVDF, respectively. This declining trend continued with an increasing number of cycles (i.e., below 10% after the fifth cycle) indicating a reduction in filtration performance. This behavior is typical for filtration membranes governed by electrostatic attraction or adsorption mechanisms [25, 26]. Initially, the dye molecules are effectively adsorbed onto the zeolite surfaces due to strong electrostatic interactions. However, as the adsorption sites become saturated during repeated cycles, the membrane's ability to capture additional dye molecules decreases, leading to a gradual decline in rejection efficiency.

The permeation flux of the pollutant filtration process was calculated using Eq. (2), as shown in Figure 2c. The PAN/PVDF membrane, serving as the control sample, exhibited significantly superior permeation flux, consistently exceeding 10,000 L m^{-2} h^{-1} bar^{-1}. This high flux indicates that the electrospun nanofiber structure inherently provides an open pore configuration, allowing efficient water flow with minimal resistance. The unmodified PAN/PVDF nanofibers, characterized by their uniform and interconnected porous network, facilitate the rapid passage of water molecules, thereby maintaining a high permeation rate throughout the filtration cycles. However, after the deposition of zeolite on the nanofiber surfaces, a notable reduction in permeation flux was observed. Among the zeolite-containing membranes, Ze50-PAN/PVDF showed the most significant decrease, with an average permeation flux of 260 ± 30 L m^{-2} h^{-1} bar^{-1} across the five filtration cycles. This pronounced decline indicates that the deposition of larger zeolite particles (50 mesh) on the nanofiber surfaces significantly reduces the availability of open pores, effectively obstructing water passage. This observation aligns with the SEM images, which show that the larger zeolite particles tend to form clusters on the membrane surface, leading to partial pore blockage.

Interestingly, the permeation flux slightly increased when finer zeolite particles were used. The average flux values for Ze100-PAN/PVDF, Ze200-PAN/PVDF, and Ze300-PAN/PVDF were recorded as 440 ± 60, 350 ± 80, and 370 ± 200 L m^{-2} h^{-1} bar^{-1}, respectively. This trend suggests that the finer zeolite particles (corresponding to higher mesh sizes) integrate more

effectively with the nanofiber matrix, preserving a greater proportion of open pores and thereby facilitating better water flow [27, 28]. The improved flux performance with decreasing particle size implies that finer zeolite particles are more compatible with the nanofiber structure, promoting better water permeability while maintaining the dye rejection capabilities.

4. CONCLUSION

In this study, we developed Ze-PAN/PVDF nanofiber membranes by incorporating natural zeolite of varying mesh sizes (50, 100, 200, and 300) through vacuum filtration. The incorporation of zeolite significantly improved dye removal efficiency compared to the pristine PAN/PVDF membrane, with Ze300-PAN/PVDF showing the most stable performance, maintaining high rejection rates (above 97%) in the first two cycles and a gradual decrease from the third cycle onward. SEM analysis revealed that smaller zeolite particles (higher mesh sizes) were more uniformly distributed within the nanofiber matrix, while larger particles formed clusters that blocked pores, reducing permeability. EDS confirmed consistent elemental composition across all samples, while FTIR analysis verified successful zeolite integration, showing characteristic Si-O-Si and Al-O-Si peaks. The permeation flux decreased significantly after zeolite deposition, with Ze50-PAN/PVDF showing the lowest flux (260 ± 30 L m^{-2} h^{-1} bar^{-1}), while finer particles (Ze300) maintained relatively higher flux (370 ± 200 L m^{-2} h^{-1} bar^{-1}). These findings highlight that optimizing zeolite particle size is crucial for balancing high dye removal efficiency and stable permeation flux, making finer zeolite particles more suitable for prolonged filtration applications.

DATA AVAILABILITY STATEMENT

The datasets generated during and/or analyzed during the current study are available from the corresponding author on reasonable request.

CONFLICT OF INTEREST

The authors declare that there are no conflicts of interest.

REFERENCES

[1] S. Y. Lee, Y. H. Tan, S. Y. Lau, N. M. Mubarak, Y. Y. Tan, I. S. Tan, Y. H. Lee, M. L. Ibrahim, R. R. Karri, M. Khalid, Y. S. Chan, J. B. Adeoye, A state-of-the-art review of metal oxide nanoflowers for wastewater treatment: Dye removal, Environmental Research 259 (2024) 119448. https://doi.org/10.1016/j.envres.2024.119448.

[2] T. A. Aragaw, A review of dye biodegradation in textile wastewater, challenges due to wastewater characteristics, and the potential of alkaliphiles, Journal of Hazardous Materials Advances 16 (2024) 100493. https://doi.org/10.1016/j.hazadv.2024.100493.

[3] J. D. Quintero A, M.- Gómez-García, I. Dobrosz-Gómez, The scope of alum coagulation-flocculation assisted by slaked lime for the treatment of industrial wastewater containing highly concentrated Acid Black 194 dye. Optimization, molecular weight distribution and toxicity analysis, Results in Engineering 23 (2024) 102676. https://doi.org/10.1016/j.rineng.2024.102676.

[4] A. Tkaczyk, K. Mitrowska, A. Posyniak, Synthetic organic dyes as contaminants of the aquatic environment and their implications for ecosystems: A review, Science of The Total Environment 717 (2020) 137222. https://doi.org/10.1016/j.scitotenv.2020.137222.

[5] M. Chebbi, S. Youcef, L. Youcef, A. Soudani, C. Dridi, A. Sahli, A. Houchet, C. Deroues, Single and combined treatment processes for rhodamine B removal by coagulation–flocculation and adsorption, RSC Advances 14 (51) (2024) 37833–37845. https://doi.org/10.1039/D4RA06882C.

[6] I. Saad, N. Ralha, M. R. Abukhadra, W. Al Zoubi, Y. G. Ko, Recent advances in photocatalytic oxidation techniques for decontamination of water, Journal of Water Process Engineering 52 (2023) 103572. https://doi.org/10.1016/j.jwpe.2023.103572.

[7] M. Homayoonfal, M. R. Mehrnia, Y. M. Mojtahedi, A. F. Ismail, Effect of metal and metal oxide nanoparticle impregnation route on structure and liquid filtration performance of polymeric nanocomposite membranes: a comprehensive review, Desalination and Water Treatment 51 (16-18) (2013) 3295–3316. https://doi.org/10.1080/19443994.2012.749055.

[8] T. Lu, J. Cui, Q. Qu, Y. Wang, J. Zhang, R. Xiong, W. Ma, C. Huang, Multistructured Electrospun Nanofibers for Air Filtration: A Review, ACS Applied Materials & Interfaces 13 (20) (2021) 23293–23313. https://doi.org/10.1021/acsami.1c06520.

[9] R. Aflaha, C. N. Maharani, L. A. Putri, Y. D. Prabowo, I. Rahman, T. Taher, A. Rianjanu, R. Roto, H. S. Wasisto, K. Triyana, A superhydrophobic and heat-resistant PAN/PSU/PTFE composite nanofiber membrane for high-efficiency $PM_{1.0}$ and $PM_{2.5}$ filtration, Materials Advances 5 (24) (2024) 9731–9743. https://doi.org/10.1039/D4MA00841C.

[10] X. Wang, B. S. Hsiao, Electrospun nanofiber membranes, Current Opinion in Chemical Engineering 12 (2016) 62–81. https://doi.org/10.1016/j.coche.2016.03.001.

[11] J. Cui, F. Li, Y. Wang, Q. Zhang, W. Ma, C. Huang, Electrospun nanofiber membranes for wastewater treatment applications, Separation and Purification Technology 250 (2020) 117116. https://doi.org/10.1016/j.seppur.2020.117116.

[12] Z. Wang, R. Sahadevan, C. Crandall, T. J. Menkhaus, H. Fong, Hot-pressed PAN/PVDF hybrid electrospun nanofiber membranes for ultrafiltration, Journal of Membrane Science 611 (2020) 118327. https://doi.org/10.1016/j.memsci.2020.118327.

[13] P. Kallem, R. Gaur, R. P. Pandey, S. W. Hasan, H. Choi, F. Banat, Thin film composite forward osmosis membranes based on thermally treated PAN hydrophilized PVDF electrospun nanofiber substrates for improved performance, Journal of Environmental Chemical Engineering 9 (5) (2021) 106240. https://doi.org/10.1016/j.jece.2021.106240.

[14] R. Nthumbi, A. Adelodun, J. Ngila, Electrospun and functionalized PVDF/PAN composite for the removal of trace metals in contaminated water, Physics and Chemistry of the Earth, Parts A/B/C 100 (2017) 225–235. https://doi.org/10.1016/j.pce.2016.08.007.

[15] Y.-J. Heo, Y. Zhang, K. Y. Rhee, S.-J. Park, Synthesis of PAN/PVDF nanofiber composites-based carbon adsorbents for CO2 capture, Composites Part B: Engineering 156 (2019) 95–99. https://doi.org/10.1016/j.compositesb.2018.08.057.

[16] X. Gao, L. Sheng, L. Yang, X. Xie, D. Li, Y. Gong, M. Cao, Y. Bai, H. Dong, G. Liu, T. Wang, X. Huang, J. He, High-stability core–shell structured PAN/PVDF nanofiber separator with excellent lithium-ion transport property for lithium-based battery, Journal of Colloid and Interface Science 636 (2023) 317–327. https://doi.org/10.1016/j.jcis.2023.01.033.

[17] M. F. Arif, S. A. Muhtar, C. Siburian, K. D. P. Marpaung, N. Yulianto, F. F. Abdi, T. Taher, H. S. Wasisto, A. Rianjanu, Zeolite-PAN/PVDF composite nanofiber membranes for highly efficient and selective removal of cationic dyes from wastewater, Case Studies in Chemical and Environmental Engineering 10 (2024) 100806. https://doi.org/10.1016/j.cscee.2024.100806.

[18] S. A. Muhtar, T. Amanda, N. R. Kurnia, S. E. M. Putra, K. Khairurrijal, M. F. Arif, T. Taher, A. Rianjanu, Complex mixture dye removal using natural zeolite modified polyacrylonitrile/polyvinylidene fluoride (Ze-PAN/PVDF) composite

nanofiber membrane via vacuum filtration technique, Materials Today Communications 42 (2025) 111357. https://doi.org/10.1016/j.mtcomm.2024.111357.

[19] S. Wang, Y. Peng, Natural zeolites as effective adsorbents in water and wastewater treatment, Chemical Engineering Journal 156 (1) (2010) 11–24. https://doi.org/10.1016/j.cej.2009.10.029.

[20] K. Bharat Jivrakh, S. Kuppireddy, S. E. Taher, K. Polychronopoulou, R. Abu Al-Rub, N. Alamoodi, G. N. Karanikolos, Zeolite-coated 3D-printed gyroid scaffolds for carbon dioxide adsorption, Separation and Purification Technology 346 (2024) 127523. https://doi.org/10.1016/j.seppur.2024.127523.

[21] S. Ma, H. Yang, S. Fu, Y. Hu, P. He, Z. Sun, X. Duan, D. Jia, P. Colombo, Y. Zhou, Additive manufacturing of hierarchical Zeolite-A lattices with exceptionally high Cs+ adsorption capacity and near-unity immobilization efficiency, Chemical Engineering Journal 474 (2023) 145909. https://doi.org/10.1016/j.cej.2023.145909.

[22] G. Başkan, Açıkel, M. Levent, Investigation of adsorption properties of oxytetracycline hydrochloride on magnetic zeolite/Fe3O4 particles, Advanced Powder Technology 33 (6) (2022) 103600. https://doi.org/10.1016/j.apt.2022.103600.

[23] Z.-d. Peng, X.-m. Lin, Y.-l. Zhang, Z. Hu, X.-j. Yang, C.-y. Chen, H.-y. Chen, Y.-t. Li, J.-j. Wang, Removal of cadmium from wastewater by magnetic zeolite synthesized from natural, low-grade molybdenum, Science of The Total Environment 772 (2021) 145355. https://doi.org/10.1016/j.scitotenv.2021.145355.

[24] L. Bandura, R. Panek, J. Madej, W. Franus, Synthesis of zeolite-carbon composites using high-carbon fly ash and their adsorption abilities towards petroleum substances, Fuel 283 (2021) 119173. https://doi.org/10.1016/j.fuel.2020.119173.

[25] Y. Zhang, H. Han, X. Wang, M. Zhang, Y. Chen, C. Zhai, H. Song, J. Deng, J. Sun, C. Zhang, Utilization of NaP zeolite synthesized with different silicon species and NaAlO2 from coal fly ash for the adsorption of Rhodamine B, Journal of Hazardous Materials 415 (2021) 125627. https://doi.org/10.1016/j.jhazmat.2021.125627.

[26] S. Zhu, J. Xu, B. Wang, J. Xie, G. Ying, J. Li, Z. Cheng, J. Li, K. Chen, Highly efficient and rapid purification of organic dye wastewater using lignin-derived hierarchical porous carbon, Journal of Colloid and Interface Science 625 (2022) 158–168. https://doi.org/10.1016/j.jcis.2022.06.019.

[27] M. Khansanami, A. Esfandiar, High flux and complete dyes removal from water by reduced graphene oxide laminate on Poly Vinylidene Fluoride/graphene oxide membranes, Environmental Research 201 (2021) 111576. https://doi.org/10.1016/j.envres.2021.111576.

[28] M. Zhu, Z. Cao, H. Yang, Z. Xu, C. Cheng, Improved dye and heavy metal ions removal in saline solutions by electric field-assisted gravity driven filtration using nanofiber membranes with asymmetric micro/nano channels, Separation and Purification Technology 300 (2022) 121775. https://doi.org/10.1016/j.seppur.2022.121775.

